

Continuous-Flow Polymerase Chain Reaction of Single-Copy DNA in Microfluidic Microdroplets

Yolanda Schaerli,^{†,‡} Robert C. Wootton,^{‡,§} Tom Robinson,[‡] Viktor Stein,[†] Christopher Dunsby,[#] Mark A. A. Neil,[#] Paul M. W. French,[#] Andrew J. deMello,[∇] Chris Abell,[‡] and Florian Hollfelder^{*†}

Department of Biochemistry and Department of Chemistry, University of Cambridge, Cambridge, U.K., and Chemical Biology Centre, Department of Chemistry, and Department of Physics, Imperial College London, London, U.K.

We present a high throughput microfluidic device for continuous-flow polymerase chain reaction (PCR) in water-in-oil droplets of nanoliter volumes. The circular design of this device allows droplets to pass through alternating temperature zones and complete 34 cycles of PCR in only 17 min, avoiding temperature cycling of the entire device. The temperatures for the applied two-temperature PCR protocol can be adjusted according to requirements of template and primers. These temperatures were determined with fluorescence lifetime imaging (FLIM) inside the droplets, exploiting the temperature-dependent fluorescence lifetime of rhodamine B. The successful amplification of an 85 base-pair long template from four different start concentrations was demonstrated. Analysis of the product by gel-electrophoresis, sequencing, and real-time PCR showed that the amplification is specific and the amplification factors of up to 5×10^6 -fold are comparable to amplification factors obtained in a benchtop PCR machine. The high efficiency allows amplification from a single molecule of DNA per droplet. This device holds promise for convenient integration with other microfluidic devices and adds a critical missing component to the laboratory-on-a-chip toolkit.

The polymerase chain reaction (PCR) is one of the most important tools in modern biology, with applications ranging from forensics to diagnostics, cloning and sequencing.¹ Normally carried out in laboratory-scale PCR cyclers, it is possible to miniaturize this process in microfluidic devices,^{2,3} reducing the cost of fabrication and consumption of biological sample, but also time of DNA amplification. Moreover, chip-based microfluidic systems are amenable to integration with other DNA processing and analysis steps in micro-

Analysis Systems (μ -TASs).^{4–6} In continuous-flow PCR, the reaction mixture passes through zones of alternating temperature corresponding to denaturation, annealing, and extension. This format avoids temperature cycling of the entire device and leads to more rapid heat transfer and faster throughput than batch PCR microfluidic chambers.⁷ However, interactions of channel walls with polymerases and template DNAs somewhat limit the biocompatibility of such systems.^{2,4,8,9} Furthermore, “-omics” applications, in which large numbers of distinct *individual* experiments are scrutinized, are hampered by potential cross-contamination as a result of deposition of DNA or proteins on channel walls.⁶ These problems can be avoided by in vitro compartmentalization of reactions in microdroplets (typically femto- to nanoliter volume) surrounded by oil serving as discrete reactors for chemical and biological reactions.^{10–12} Such reactors allow separate handling of members of large combinatorial libraries in microfluidic devices. Droplets can be formed,^{13–15} divided,^{16,17} fused,^{18–20} incubated,^{21–23} and sorted^{17,18,24} potentially creating an integrated system for biological experimentation with a level of control akin to experiments on the macroscopic scale. Compartmentalization of experiments can also improve on those carried out in the usual fashion. For example, performing PCR in emulsions has been shown to avoid preferential amplification of short sequences and of artifactual fragments generated by recombination between homologous regions of DNA, thus resolving two problems hindering the amplification of complex mixtures of genes by PCR in solution.²⁵

* To whom correspondence should be addressed. E-mail: fh111@cam.ac.uk. Phone: +44 1223 766 048. Fax: +44 1223 766 002.

[†] Department of Biochemistry, University of Cambridge.

[‡] Department of Chemistry, University of Cambridge.

[§] Current address: School of Pharmacy and Chemistry, Liverpool John Moores University, Liverpool, U.K.

[∇] Chemical Biology Centre, Imperial College London.

[#] Department of Physics, Imperial College London.

[∇] Department of Chemistry, Imperial College London.

(1) Mullis, K.; Faloona, F.; Scharf, S.; Saiki, R.; Horn, G.; Erlich, H. *Cold Spring Harbor Symp. Quant. Biol.* **1986**, *51*, 263–273.

(2) Zhang, C.; Xu, J.; Ma, W.; Zheng, W. *Biotechnol. Adv.* **2006**, *24*, 243–284.

(3) deMello, A. J. *Nature* **2003**, *422*, 28–29.

(4) Auroux, P.-A.; Koc, Y.; deMello, A.; Manz, A.; Day, P. J. R. *Lab Chip* **2004**, *4*, 534–546.

(5) Chen, L.; Manz, A.; Day, P. J. R. *Lab Chip* **2007**, *7*, 1413–1423.

(6) Zhang, C.; Xing, D. *Nucleic Acids Res.* **2007**, *35*, 4223–4237.

(7) Kopp, M. U.; J.deMello, A. J.; Manz, A. *Science* **1998**, *280*, 1046–1048.

(8) Krishnan, M.; Burke, D. T.; Burns, M. A. *Anal. Chem.* **2004**, *76*, 6588–6593.

(9) deMello, A. J. *Lab Chip* **2001**, *1*, 24N–29N.

(10) Griffiths, A. D.; Tawfik, D. S. *Trends Biotechnol.* **2006**, *24*, 395–402.

(11) Taly, V.; Kelly, B. T.; Griffiths, A. D. *ChemBioChem* **2007**, *8*, 263–272.

(12) Kelly, B. T.; Baret, J.-C.; Taly, V.; Griffiths, A. D. *Chem. Commun.* **2007**, *1773*, 1788.

(13) Anna, S. L.; Bontoux, N.; Stone, H. A. *Appl. Phys. Lett.* **2003**, *82*, 364–366.

(14) Tan, Y.-C.; Cristini, V.; Lee, A. P. *Sens. Actuators, B Chem.* **2006**, *114*, 350–356.

(15) Thorsen, T.; Roberts, R. W.; Arnold, F. H.; Quake, S. R. *Phys. Rev. Lett.* **2001**, *86*, 4163–4166.

(16) Link, D. R.; Anna, S. L.; Weitz, D. A.; Stone, H. A. *Phys. Rev. Lett.* **2004**, *92*, 054503.

(17) Link, D. R.; Grasland-Mongrain, E.; Duri, A.; Sarrazin, F.; Cheng, Z.; Cristobal, G.; Marquez, M.; Weitz, D. A. *Angew. Chem.* **2006**, *118*, 2618–2622.

(18) Ahn, K.; Kerbage, C.; Hunt, T. P.; Westervelt, R. M.; Link, D. R.; Weitz, D. A. *Appl. Phys. Lett.* **2006**, *88*, 024104.

(19) Fidalgo, L. M.; Abell, C.; Huck, W. T. S. *Lab Chip* **2007**, *7*, 984–986.

In contrast to emulsion formation in bulk,^{26,27} the well-defined size of droplets formed in microfluidics allows quantitative assays.^{21,23,28–31} Integration of such an assay platform with DNA amplification and *in vitro* expression^{21,22} would allow the analysis of genomic libraries, cDNA libraries, and man-made DNA libraries. In addition assays for medical diagnostics and microbial detection involving DNA amplification can be carried out in this manner, with the compartmentalization of the DNA amplification giving rise to a digital readout that can be interpreted by statistical analysis.^{32–34}

To achieve the high-throughput necessary for all these potential applications, continuous processing of droplet reactors is crucial, but the current set-ups for PCR in microfluidic microdroplets have involved thermal cycling of the entire device, thus limiting throughput.^{33,34} PCR in moving microliter droplets has been described,^{35,36} but the use of such large droplets reduces throughput and is not simply integrated with current microfluidic devices.^{10–12} PCR has also been performed in droplets containing paramagnetic particles that can be moved by magnetic forces, but the throughput of these methods is again limited.^{37,38}

In this paper we describe a microfluidic device for continuous-flow PCR in microfluidic water-in-oil nanoliter droplets. The droplets flow through alternating temperature zones in a radial pattern for denaturation of the DNA and annealing of the primer/extension of the template. Temperature measurements inside the droplets confirmed that the applied settings are adequate for PCR. Highly efficient amplification was achieved even at low template concentrations where most of the droplets either contain no or only one template.

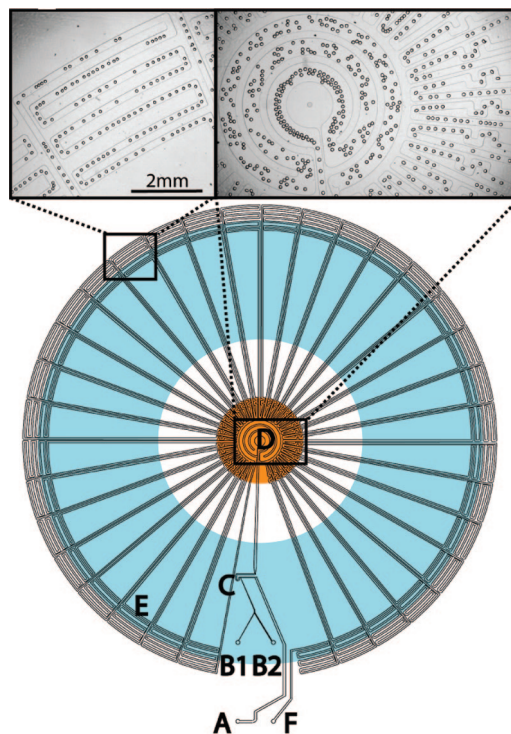


Figure 1. Design of the radial PCR device. The device contains an oil inlet (A) that joins two aqueous inlet channels (B1 and B2) to form droplets at a T-junction (C). The droplets pass through the inner circles (500 μm wide channels) in the hot zone (D) to ensure initial denaturation of the template and travel on to the periphery in 200 μm wide channels where primer annealing and template extension occur (E). The droplets then flow back to the center, where the DNA is denatured and a new cycle begins. Finally, the droplets exit the device after 34 cycles (F). All channels are 75 μm deep. The positions of the underlying copper rod (\varnothing : 1.2 cm) and the Peltier module (inner \varnothing : 2.7 cm, outer \varnothing : 5.5 cm) are indicated with orange and blue areas, respectively. Devices are made of SU-8 embedded in PMMA.

EXPERIMENTAL SECTION

Device Design and Material. Devices with 75 μm deep and 200–500 μm wide channels were used (Figure 1). These were fabricated by Epigem Ltd. from films of SU-8. The SU-8 substrate was photocross-linked and non cross-linked areas removed by chemical developers. The SU-8 substrate was embedded in a PMMA support matrix to provide structural strength. The resulting channel network was closed using a thermal bonding protocol developed by Epigem Ltd. and linked to the tubing by a ferrule-based interface clamp. The heater consisted of a 1.2 cm wide copper rod with a 100 W cartridge heater (RS components) thermostatically controlled via a J type thermocouple. External adjustment of thermal gradient was via an annular Peltier module 15 W (Melcor). The heater was supported on an aluminum heat sink that was itself cooled by four thermoelectric heat pumps mounted with fan-cooled heat exchangers (Maplin). The contact between the device and the heater was ensured by a thin film of heat sink compound (RS components).

Device Operation. The solutions were in glass syringes (500 and 1000 μL Hamilton Gastight syringes), and the flow was driven using Harvard Apparatus 2000 syringe infusion pumps. Typical total flow rates were around 160 $\mu\text{L}/\text{h}$; the choice of the ratio between the aqueous and the oil flow rates was guided by the desired droplet size. Pictures and movies were recorded with a Phantom V72 camera. Image analysis to determine the size and frequency of the droplets

- (20) Tan, Y.-C.; Fisher, J. S.; Lee, A. I.; Cristini, V.; Lee, A. P. *Lab Chip* **2004**, *4*, 292–298.
- (21) Courtois, F.; Olguin, L. F.; Whyte, G.; Bratton, D.; Huck, W. T. S.; Abell, C.; Hollfelder, F. *ChemBioChem* **2008**, *9*, 439–446.
- (22) Dittrich, P. S.; Jahnz, M.; Schwille, P. *ChemBioChem* **2005**, *6*, 811–814.
- (23) Clausell-Tormos, J.; Lieber, D.; Baret, J.-C.; El-Harrak, A.; Miller, O. J.; Frenz, L.; Blouwolf, J.; Humphry, K. J.; Köster, S.; Duan, H.; Holtze, C.; Weitz, D. A.; Griffiths, A. D.; Merten, C. A. *Chem. Biol.* **2008**, *15*, 427–437.
- (24) Fidalgo, L.; Whyte, G.; Bratton, D.; Kaminski, C.; Abell, C.; Huck, W. *Angew. Chem., Int. Ed. Engl.* **2008**, *47*, 2042–2045.
- (25) Williams, R.; Peisajovich, S. G.; Miller, O. J.; Magdassi, S.; Tawfik, D. S.; Griffiths, A. D. *Nat. Methods* **2006**, *3*, 545–550.
- (26) Miller, O. J.; Bernath, K.; Agresti, J. J.; Amitai, G.; Kelly, B. T.; Mastrobattista, E.; Taly, V.; Magdassi, S.; Tawfik, D. S.; Griffiths, A. D. *Nat. Methods* **2006**, *3*, 561–570.
- (27) Ghadessy, F. J.; Holliger, P. *Methods Mol. Biol.* **2007**, *352*, 237–248.
- (28) Song, H.; Ismagilov, R. F. *J. Am. Chem. Soc.* **2003**, *125*, 14613–14619.
- (29) Huebner, A.; Olguin, L. F.; Bratton, D.; Whyte, G.; Huck, W. T. S.; de Mello, A. J.; Edel, J. B.; Abell, C.; Hollfelder, F. *Anal. Chem.* **2008**, *80*, 3890–3896.
- (30) Huebner, A.; Srisa-Art, M.; Holt, D.; Abell, C.; Hollfelder, F.; deMello, A. J.; Edel, J. B. *Chem. Commun.* **2007**, *1218*, 1220.
- (31) Srisa-Art, M.; deMello, A. J.; Edel, J. B. *Anal. Chem.* **2007**, *79*, 6682–6689.
- (32) Vogelstein, B.; Kinzler, K. W. *Proc. Natl. Acad. Sci. U.S.A.* **1999**, *96*, 9236–9241.
- (33) Beer, N. R.; Hindson, B. J.; Wheeler, E. K.; Hall, S. B.; Rose, K. A.; Kennedy, I. M.; Colston, B. W. *Anal. Chem.* **2007**, *79*, 8471–8475.
- (34) Beer, N.; Wheeler, E.; Lee-Houghton, L.; Watkins, N.; Nasarabadi, S.; Hebert, N.; Leung, P.; Arnold, D.; Bailey, C.; Colston, B. *Anal. Chem.* **2008**, *80*, 1854–1858.
- (35) Dorfman, K. D.; Chabert, M.; Codarbox, J.-H.; Rousseau, G.; de Cremoux, P.; Viovy, J.-L. *Anal. Chem.* **2005**, *77*, 3700–3704.
- (36) Chabert, M.; Dorfman, K. D.; de Cremoux, P.; Roeraade, J.; Viovy, J.-L. *Anal. Chem.* **2006**, *78*, 7722–7728.
- (37) Ohashi, T.; Kuyama, H.; Hanafusa, N.; Togawa, Y. *Biomed. Microdevices* **2007**, *9*, 695–702.
- (38) Pipper, J.; Inoue, M.; Ng, L. F.-P.; Neuzil, P.; Zhang, Y.; Novak, L. *Nat. Med.* **2007**, *13*, 1259–1263.

was performed with software written with LabView 8.2.²¹ The volumes of the droplets were calculated from the equation $V = 4/3\pi r^3$ for the volume of a sphere. This was only done for droplets with a diameter smaller than the channel depth (75 μm). Residence times of the droplets per cycle and in the entire device were measured by following droplets by eye and stopping the time.

Two aqueous phases were injected: one containing the polymerase, buffer, and bovine serum albumin (BSA), the other containing the DNA template, primers, deoxynucleotides (dNTPs), MgCl_2 , buffer, and BSA.

PCR Reagents. The final PCR mixture contained 0.1 U/ μL BioTaq DNA polymerase (BioLine), BioTaq PCR NH_4 -based reaction buffer, 2 mM MgCl_2 (BioLine), 0.25 mM dNTPs each (BioLine), 100 $\mu\text{g}/\text{mL}$ BSA (New England Biolabs), 2 μM primers (5'-ACTCACCCACCCCAGAGCG-3', 5'-ATTTGTTUACCAAGGGT-GCGGAGG-3') (Operon) amplifying a 85 bp sequence of the tyrocidine synthetase 1 gene (P09095) and specified amounts of template. The carrier fluid was 3% (w/w) ABIL EM90 (Goldschmidt GmbH) in light mineral oil (Sigma). All solutions were filtered (0.2 μm) before use.

Product Analysis. Droplets were collected in a tube until 25 μL of the aqueous phase was collected. The emulsions were centrifuged for 5 min at 13,000 g and the upper oil phase was removed. The remaining oil was extracted twice by addition of water-saturated diethyl ether (1 mL), vortexing the tube, and disposing of the upper, organic phase. Residual diethyl ether was removed by centrifuging under vacuum for 5 min at 25 $^\circ\text{C}$.

The amplification factors were determined by RT-PCR on a Rotor-Gene 6000 (Corbett) using SYBR Green I (Quantace) as detection dye. DNA amounts were determined relative to a standard ladder. The amplification factor was calculated by comparing the amount of DNA in the collected aqueous phase relative to the measured input value. SensiMix *NoRef* Kit (Quantace) was used according to the manufacturer's instructions. The total reaction volume was 25 μL and included 2 μL of sample. The same primers as for the amplification on chip were used at a concentration of 200 nM. The thermal cycling conditions were 95 $^\circ\text{C}$ for 10 min followed by 40 cycles of 15 s at 60 $^\circ\text{C}$, 20 s at 72 $^\circ\text{C}$, and 10 s at 95 $^\circ\text{C}$. Measurements were performed in triplicates for each sample. The real-time trace, standard ladder and gel can be found in the Figure S5, Supporting Information.

Sequencing. The 85 bp long product of the PCR performed in microfluidic microdroplets and in a benchtop PCR machine was cloned into a pCR4-TOPO vector with a TOPO TA cloning kit for sequencing (Invitrogen) according to the manufacturer's instructions. Ten clones of each cloning reaction were picked, grown as an overnight culture, and the plasmids were isolated with a miniprep kit (Sigma). The plasmids were sequenced (Applied Biosystems 3730xl DNA Analyzer, DNA sequencing facility, Department of Biochemistry, University of Cambridge, U.K.) with the M13 reverse primer.

FLIM. A 500 μM solution of Rhodamine B in 50 mM Tris/HCl, pH 6.8 was used to form aqueous droplets in mineral oil containing 3% (w/w) ABIL EM90. The fluorescence lifetime was measured with a confocal microscope (Leica SP5) using supercontinuum laser generation as the excitation source³⁹ and time-correlated single

photon counting detection⁴⁰ over a time of 3 min. The temperatures were obtained from the fluorescence decay time via a calibration curve (Figure S3, Supporting Information).

RESULTS AND DISCUSSION

Figure 1 shows the device design for single-copy continuous-flow PCR in water-in-oil droplets (tunable \varnothing of 40–150 μm). The device is made of SU-8 embedded in a poly(methyl methacrylate) (PMMA) support matrix. Droplets are formed at a T-junction¹⁵ and run through zones of varying temperatures. Our radial design features a central hot zone (brought about by a heated copper rod; \varnothing : 1.2 cm) for initial template denaturation in the three central circular channels. Heating from the center establishes a natural temperature gradient across the device. The increasingly lower temperatures experienced as the droplet travels to the periphery of the device allow annealing of the primers to the denatured DNA and their extension by the DNA polymerase. Seven loops increase the residence time of the droplets in the annealing/extension temperature zone in a two-temperature PCR protocol.⁴¹ The droplets are then led back to the center, to initiate a new cycle (Movie S1, Supporting Information). By exploiting the natural temperature gradient across the device there is no need to thermally isolate different temperature zones to produce an annular continuous temperature distribution.⁴² The gradient can be externally adjusted via an annular Peltier module that can be heated or cooled according to requirements of the template and primers. The droplets were stabilized by the addition of 3% ABIL EM90 surfactant to the mineral oil,^{21,43} so that they remained intact even at high temperatures (Movies S2, Supporting Information). A previously reported formulation (4.5% Span 80, 0.4% Tween 80 and 0.05% Triton X-100 in mineral oil)⁴⁴ was also tested, but droplets coalesced at high temperatures. The devices were not susceptible to failure when heated and run for several days.

Precise temperature control is important for successful DNA amplification by PCR. To this end fluorescence lifetime imaging (FLIM) was used to measure the temperature inside the droplets, exploiting the temperature-dependent fluorescence lifetime of rhodamine B.⁴⁵ FLIM can provide robust quantitative temperature mapping with high spatial resolution by extracting fluidic temperatures from the fluorescence decay time via a single calibration curve (Figure S3, Supporting Information). Unlike measurements of time-integrated fluorescence intensity FLIM is independent of experimental parameters such as dye concentration and excitation or detection efficiency. Rhodamine B was incorporated in the aqueous droplets (but not in the oil phase) to monitor the temperature inside moving droplets. FLIM was undertaken using a confocal microscope (Leica SP5) with supercontinuum laser generation as the excitation source³⁹ and time-correlated single photon counting detection.⁴⁰ Figure 2 illustrates representative FLIM data in the denaturation zone located in the device center (Figure 2a) and in the annealing/

(40) Becker, W. *Advanced time-correlated single photon counting techniques*; Springer: Berlin, 2005.

(41) Lopez, J.; Prezioso, V. *Eppendorf BioNews Appl. Notes* **2001**, *16*, 3–4.

(42) Cheng, J.-Y.; Hsieh, C.-J.; Chuang, Y.-C.; Hsieh, J.-R. *Analyst* **2005**, *130*, 931–940.

(43) Diehl, F.; Li, M.; Dressman, D.; He, Y.; Shen, D.; Szabo, S.; Diaz, L. A.; Goodman, S. N.; David, K. A.; Juhl, H.; Kinzler, K. W.; Vogelstein, B. *Proc. Natl. Acad. Sci. U.S.A.* **2005**, *102*, 16368–16373.

(44) Dressman, D.; Yan, H.; Traverso, G.; Kinzler, K. W.; Vogelstein, B. *Proc. Natl. Acad. Sci. U.S.A.* **2003**, *100*, 8817–8822.

(45) Benninger, R. K. P.; Koç, Y.; Hofmann, O.; Requejo-Isidro, J.; Neil, M. A. A.; French, P. M. W.; deMello, A. J. *Anal. Chem.* **2006**, *78*, 2272–2278.

(39) Dunsby, C.; Lanigan, P. M. P.; McGinty, J.; Elson, D. S.; Requejo-Isidro, J.; Munro, I.; Galletly, N.; McCann, F.; Treanor, B.; Onfelt, B.; Davis, D. M.; Neil, M. A. A.; French, P. M. W. *J. Phys. D: Appl. Phys.* **2004**, *37*, 3296–3303.

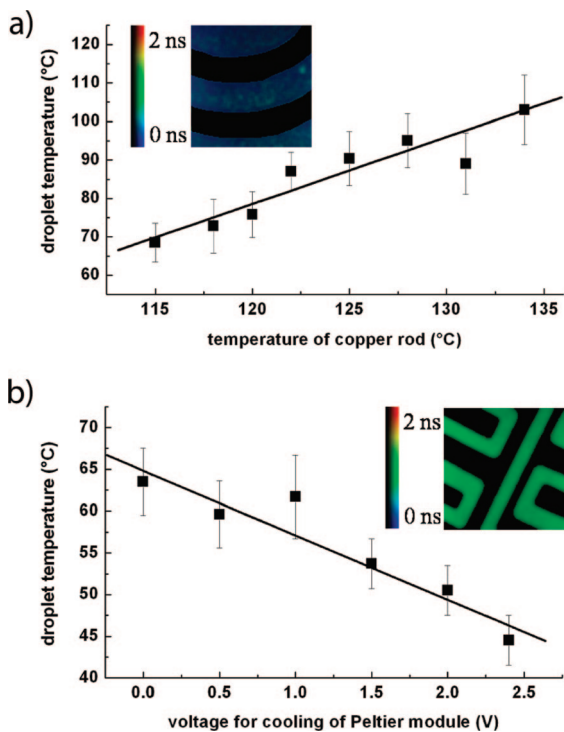


Figure 2. Fluorescence lifetime data from droplets containing 500 μM rhodamine B and flowing in the channels at total volumetric flow rate of 120 $\mu\text{L/h}$. (a) Temperatures of droplets determined from FLIM data (using the calibration curve in Figure S3, Supporting Information) in the denaturation zone (device center) as a function of the heating copper rod temperature. The Peltier module was turned off. Inset: false-color-scale map of the mean fluorescence-decay time measured at 94 °C (304 ps). (b) Temperatures of droplets determined from FLIM data in the annealing and extension zone (device periphery) as a function of the voltage for the cooling of the Peltier module. The copper rod was set to 134 °C. Inset: false-color-scale map of the mean fluorescence-decay time measured at 49 °C (853 ps). Error bars were calculated from the standard deviation of the fluorescence lifetime. The straight lines represent linear fits.

extension zone at the periphery (Figure 2b). The device design allows for adjustment of these temperatures to match specific requirements of the template and primers by heating the copper rod and cooling or heating of the Peltier module. The transition from the high temperature to the lower temperature for annealing/extension is fast as a temperature profile of the device shows (Figure S4, Supporting Information).

An 85 bp sequence, a typical amplicon length for quantitative PCR, was amplified and analyzed by gel electrophoresis. Figure 3a shows one clear band per lane providing evidence that the PCR produced only the desired product.

The amplification factor (i.e., the product yield with respect to the starting concentration) was determined by real-time (RT) PCR. Figure 3b describes the relationship between the template concentration (ranging between 0 and 46 pM) and the amplification factor. The amplification factor increased with decreasing template concentration up to 5×10^6 , and a product concentration of 63–167 nM was reached in droplets. This is 3 orders of magnitude lower than the theoretical maximal amplification factor of 1.7×10^{10} ($= 2^{34}$) for exponential amplification over 34 cycles. In practice, however, amplification yields are lower as the amplification is not exponential until the end of the PCR, but reaches a plateau at a relatively constant level of product that is largely independent of

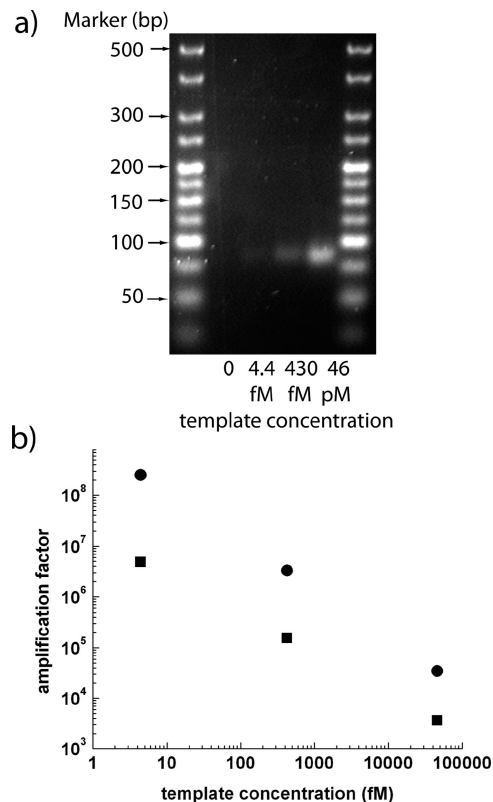


Figure 3. Analysis of PCR products. (a) Gel electrophoresis of the PCR products obtained by continuous-flow PCR in microdroplets. The 85 bp sequence was amplified in droplets of an average diameter of 63 μm and with a calculated volume of 131 pL. A total volumetric flow rate of 160 $\mu\text{L/h}$ was used resulting in 17 min residence time of the droplets in the device. The copper rod was set to 134 °C, and the Peltier module was cooled with 1 V. 10^4 – 10^6 droplets were collected at the device outlet, broken up, and 15 μL of the aqueous phase were run on an ethidium bromide stained 3% agarose gel. Marker: Hyperladder V (Biolone). (b) Amplification factors were determined by RT-PCR and plotted against the starting concentration of DNA template. The corresponding average number of starting templates per droplet were 0, 0.3, 34, and 3600. The data obtained in microfluidic microdroplets (■) were compared to amplification factors achieved in solution in a commercial thermocycler (●) under identical conditions with a cycling time of 67 min (2 min at 94 °C, followed by 34 cycles of 15 s at 94 °C and 30 s at 55 °C). The aqueous phases recovered as described above, were diluted 1000-fold, and the amount of the 85 bp DNA amplicon was determined by RT-PCR (Figure S5, Supporting Information).

the starting concentration. A number of experimental factors have been discussed to contribute to the attenuation in the exponential amplification, including product inhibition and template rehybridization.^{9,46} For comparison amplification factors achieved in solution in an Eppendorf thermocycler, were only 9–52 fold higher than the amplification achieved in microfluidic droplets (Figure 3b).

The integrity of the product was also verified by sequencing. The product of the PCR performed in microfluidic microdroplets and in a benchtop PCR machine was cloned into a pCR4-TOPO vector with a TOPO TA cloning kit for sequencing. Ten clones of each cloning reaction were picked, grown as an overnight culture, and the plasmids were isolated and sequenced. Nine clones originated from microfluidic microdroplets amplification products were identical with the template, one clone contained a single point mutation (adenine to guanine). For the amplification products from the benchtop PCR

(46) Kainz, P. *Biochim. Biophys. Acta* 2000, 1494, 23–27.

machine were also nine clones error-free and one clone contained a one-base (guanine) insertion. This indicates that the error rate of the Taq polymerase was not increased in microfluidic microdroplets compared to PCR carried out in solution in a benchtop machine. A representative sequencing result is shown in Figure S6, Supporting Information.

The observation that very high amplification could be achieved suggests that the polymerase remains active during its transit through the device. In contrast to microfluidics without compartmentalization, where adsorption of the polymerase onto the device walls^{2,4,8,9} and chemical inhibition of the PCR by the device material⁴⁷ are frequently encountered problems, the PCR ingredients are in direct contact with the device material only for a very short period prior to droplet formation.

Dilution of DNA template relative to the droplet number showed that we were able to amplify DNA in droplets containing a single-copy template: 4.4 fM template concentration corresponds to 0.3 templates per 131 pL droplet, resulting in 74.1% empty droplets, 22.2% droplets containing one template, and 3.3% droplets containing two templates according to a Poisson distribution. It has previously been shown, that DNA in microfluidic droplets is Poisson distributed.^{21,33,34} The proportionate increase of the amplification factor dependent on the starting concentration (Figure 3b) also suggests that single copies are amplified as efficiently as if several copies were in a droplet.

The ability to amplify DNA in “monoclonal” droplets is a pivotal result paving the way for a variety of possible future applications. These include, for example, digital PCR,^{32–34,48} once combined with an online detection system.⁴⁹ Digital PCR transforms exponential analog data from conventional PCR to more reliable linear digital signals that show whether or not amplification has occurred and hence whether or not the template was present. By using the Poisson distribution this allows the detection and quantification of very low concentrations of a sequence in a complex DNA mixture such as encountered in medical diagnostics and microbial detection. It also allows for many more applications such as identification of predefined mutations³² or cells carrying a particular gene.⁴⁸ In digital PCR the limit of detection is defined by the number of compartments,³² so continuous systems will provide better data than batch methods with lower throughput.

Preliminary experiments suggest that our system could also be used to amplify templates long enough to code for small proteins, although further optimization might be necessary to achieve more efficient amplification of long templates (Figure S7, Supporting Information). Currently the 505 bp fragment amplification is about 20-fold less efficient than the amplification of an 85 bp fragment at

the starting concentration tested (1 nM). The ability to adjust temperatures in droplets via the copper rod and the Peltier module, as well as the possibility to measure them inside the droplets by FLIM, will enable optimization of the temperature profile by decreasing the formation of potential side products (e.g., primer dimer) and improving the current amplification factor for longer templates. In addition the residence times of the droplets in the different temperatures zones can also be straightforwardly adjusted by changing the flow rates and/or the path length in the different zones.

Amplification of sequences coding for proteins would eventually be useful for application of a PCR device in directed evolution experiments in microdroplets¹⁰ where a library of different DNA templates is expressed in vitro and screened for a desired activity. PCR in droplets will make this process more efficient, as template amplification results in increased protein expression leading to increased sensitivity of detection and ultimately to higher recovery and enrichment rates.

Our device was typically operated at a total volumetric flow rate of 160 $\mu\text{L}/\text{h}$, resulting in a droplet formation frequency of 15 Hz and a residence time of 29 s per PCR cycle. The high throughput of 10^6 droplets per day achieved in this continuous-flow PCR can be interfaced directly with incubation, sorting, and analysis. By comparison thermal cycling of stationary droplets on the device^{33,34} or collecting microfluidic droplets and subjecting them to thermal cycling in a benchtop PCR machine⁵⁰ only allows sampling of a smaller number of droplets, and integration with downstream microfluidic elements is far from convenient.

CONCLUSION

Single-copy PCR in droplets as the biomimetic equivalent of archetypal protocells provides a route for DNA amplification as basic evolutionary units that combine genotype and phenotype. The ability to integrate a PCR module adds a critical missing component to the laboratory-on-a-chip toolkit and provides that the basis for integrated systems for biological experimentation including a future chip-based evolution machine and a high-throughput digital PCR device.

ACKNOWLEDGMENT

We acknowledge P. Summersgill of Epigem, L. M. Fidalgo and G. Whyte for their help. This work was supported by the RCUK Basic Technology Programme, the EU NEST project MiFem, a Department of Trade and Industry (DTI) Beacon award Sciences Research Council (EPSRC). Y.S. thanks the Schering Foundation for a fellowship and the Cambridge Overseas Trust and Trinity Hall, Cambridge for support. V.S. was supported by a studentship of Trinity College, Cambridge, and the Biotechnology and Biological Sciences Research Council (BBSRC). F.H. is an ERC Starting Investigator.

SUPPORTING INFORMATION AVAILABLE

Additional information as noted in the text. This material is available free of charge via the Internet at <http://pubs.acs.org>.

Received for review September 25, 2008. Accepted November 6, 2008.

AC802038C

(47) Shoffner, M. A.; Cheng, J.; Hvichia, G. E.; Kricka, L. J.; Wilding, P. *Nucleic Acids Res.* **1996**, *24*, 375–379.

(48) Ottesen, E. A.; Hong, J. W.; Quake, S. R.; Leadbetter, J. R. *Science* **2006**, *314*, 1464–1467.

(49) Kumaresan, P.; Yang, C. J.; Cronier, S. A.; Blazej, R. G.; Mathies, R. A. *Anal. Chem.* **2008**, *80*, 3522–3529.

(50) After the submission of this paper Kiss et al. published an online detection system in which a range of template concentrations could be detected by continuous-flow digital PCR that agreed with the frequencies predicted by Poisson statistics: Kiss, M. M.; Ortoleva-Donnelly, L.; Beer, N. R.; Warner, J.; Bailey, C. G.; Colston, B. W.; Rothberg, J. M.; Link, D. R.; Leamon, J. H. *Anal. Chem.* **2008**, *80*, 8975–8981.